

Kinetic study on carbonation of crude Li_2CO_3 with CO_2 -water solutions in a slurry bubble column reactor

Wen-Tao Yi*†, Chun-Yan Yan*, and Pei-Hua Ma**

*Department of Chemistry and Chemical Engineering, Zaozhuang University, Zaozhuang 277160, China

**Qinghai Institute of Salt Lakes, Chinese Academy of Sciences, Xining 810008, China

(Received 13 April 2010 • accepted 19 August 2010)

Abstract—Investigations were conducted to purify crude Li_2CO_3 via direct carbonation with CO_2 -water solutions at atmospheric pressure. The experiments were carried out in a slurry bubble column reactor with 0.05 m inner diameter and 1.0 m height. Parameters that may affect the dissolution of Li_2CO_3 in the CO_2 -water solutions such as CO_2 -bubble perforation diameter, CO_2 partial pressure, CO_2 gas flow rate, Li_2CO_3 particle size, solid concentration in the slurry, reaction temperature, slurry height in the column and so on were investigated. It was found that the increases of CO_2 partial pressure, and CO_2 flow rate were favorable to the dissolution of Li_2CO_3 , which had the opposite effects with Li_2CO_3 particle size, solid concentration, slurry height in the column and temperature. On the other hand, in order to get insight into the mechanism of the refining process, reaction kinetics was studied. The results showed that the kinetics of the carbonation process can be properly represented by $1-3(1-X)^{2/3}+2(1-X)=kt+b$, and the rate-determining step of this process under the conditions studied was product layer diffusion. Finally, the apparent activation energy of the carbonation reaction was obtained by calculation. This study will provide theoretical basis for the reactor design and the optimization of the process operation.

Key words: Carbonation, Kinetics, Slurry Bubble Column Reactor, Crude Li_2CO_3 , Mechanism

INTRODUCTION

High purity Li_2CO_3 can be used for the production of medicines, electronic grade crystals, such as LiNbO_3 and LiTaO_3 crystals, and high purity lithium metal. With the development of batteries and single crystal industries in the world, the demand for it has been dramatically growing in recent years, but its supply is to some degree insufficient. Therefore, improving the production of high purity Li_2CO_3 is extremely necessary nowadays. Attempts to produce high purity Li_2CO_3 were made by Brown et al. as early as the 1970s [1,2]. There exist abundant in lithium resources with large reserves in China which provide relatively low-cost feedstock to prepare high purity Li_2CO_3 . The work aimed at purifying Li_2CO_3 from such feedstock via its slurry phase dissolution in a slurry bubble column reactor.

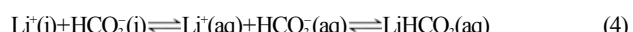
Commercial crude Li_2CO_3 produced from lithium-containing minerals, brines or sea water carries considerable amounts of impurities, such as calcium, magnesium and other multivalent ions as well as acid insoluble residues and so on. To eliminate them, the slight-soluble Li_2CO_3 should be first converted to a water-soluble compound. Direct carbonation of Li_2CO_3 by pure CO_2 will not introduce other impurities, and water-soluble LiHCO_3 can be obtained; secondly, and no less important, CO_2 as a leaching agent has almost no appreciable environmental impact because the residues can be recycled for further use. Impurities in the crude Li_2CO_3 are either solubilized or precipitated out. The dissolved impurities are separated from LiHCO_3 solution by means of ion exchange, or liquid-liquid extraction. High purity Li_2CO_3 is then precipitated out by heating the purified LiHCO_3 .

solution under vacuum [3-6]. Clearly, the carbonation stage is very important in controlling the production rate of high purity Li_2CO_3 . Therefore, it is very necessary to know the carbonation mechanism and its kinetics. The mechanisms and kinetics of the carbonation of CaO and MgO with similar process have been reported [7,8]. And the carbonation of limestone, K_2CO_3 and Rb_2CO_3 for CO_2 capture has also been investigated [9-11]. The slurry bubble column reactor has been widely used in a number of chemical, biochemical and environmental processes, because of its many advantages over other multiphase reactors, such as simple construction, good mass transfer properties, high thermal stability, low energy supply and hence low construction and operation costs. However, the kinetics of this stage in a slurry bubble column reactor at atmospheric pressure in particular has never been reported until now. For uncatalyzed reactions, a correlation exists between the kinetics and the reaction conditions, so it is very vital to investigate this part from the view of theory and practice.

In this work, extensive investigations have been carried out to elucidate the mechanism of carbonation of Li_2CO_3 slurries. The total reaction of the process can be expressed by Eq. (1), and it is a gas-liquid-solid three phase reaction.



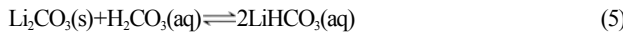
The main reactions involved in the process are as follows:



or, by summation

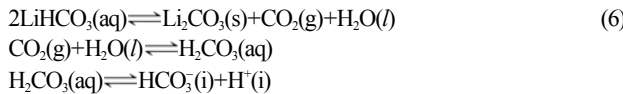
†To whom correspondence should be addressed.

E-mail: casqisl@163.com



where $\text{HCO}_3^-(\text{i})$, $\text{H}^+(\text{i})$ and $\text{Li}^+(\text{i})$ are the products formed and/or adsorbed at the interface.

The recovery of CO_2 and production of pure Li_2CO_3 precipitate can be accomplished by heating the purified lithium bicarbonate solution under vacuum conditions. The precipitation process (see Eq. (6)) is conducted at 353 K and 0.035 MPa, which will not be further covered in this paper.



The dissolution rate of any mineral is dependent upon the transport rate of reactants and products between the mineral surface and the bulk solution, the rate of heterogeneous reaction at the mineral surface, and, possibly, on the rates of homogeneous reactions within the solution [12].

The reaction rate constants of the first part of Eq. (2), i.e., $\text{CO}_2(\text{g}) + \text{H}_2\text{O}(\text{l}) \rightleftharpoons \text{H}_2\text{CO}_3(\text{aq})$ at 1 atm and 298 K as found by Loewenthal and Maria are 0.037 s^{-1} for the forward reaction and 13.7 s^{-1} for the backward reaction [13]. This means that the forward reaction is slow while the backward reaction is much faster. On the other hand, the reaction rate constants for the second part of Eq. (2), i.e., $\text{H}_2\text{CO}_3(\text{aq}) \rightleftharpoons \text{HCO}_3^-(\text{i}) + \text{H}^+(\text{i})$, are far larger than those of other reactions involved in Eq. (2) [14]. As a result, for the hydration of CO_2 in plain water, the whole reaction (2) is in equilibrium. But in this process, the hydrogen ions formed in Eq. (2) react with the $\text{Li}_2\text{CO}_3(\text{s})$ in the slurry; thus the reaction moves forward and more bicarbonate ions are formed. Clearly, the dissolution of CO_2 is vital for the progress of this process. However, it is reported that the dissolution of CO_2 in electrolyte solution decreases with increasing the ionic strength in the solution, and the relationship between the CO_2 solubility coefficient and the ionic strength can be approximately defined by Van Krevelen and Hoflyzer correlation, as shown in the form of Eq. (7) [15].

$$\log(H_0/H) = h_1 I_1 + h_2 I_2 + \dots \quad (7)$$

where H_0 and H are the solubility coefficients of CO_2 in plain water and electrolyte solution, respectively; I_1 and I_2 are the ionic strengths of the electrolytes, $I = 0.5a c Z_i^2$, in which c_i is the ion concentration and Z_i is the ionic valence; h_1, h_2, \dots are the reduced coefficients of the CO_2 solubility induced by the electrolyte in the solution, and it

Table 1. h_G of CO_2 at different temperatures

T/K	273	288	298	313	323
h_G	-0.007	-0.010	-0.019	-0.026	-0.029

Table 2. h_+ and h_- Values of the common ions

	$h_+ / \text{m}^3 \cdot \text{kg}_{\text{ion}}^{-1}$	$h_- / \text{m}^3 \cdot \text{kg}_{\text{ion}}^{-1}$
H^+	0.000	0.066
Na^+	0.091	0.119
K^+	0.074	0.021
Ca^{2+}	0.053	0.021
Mg^{2+}	0.051	0.022

Table 3. The solubility of Li_2CO_3 in water at different temperatures (Solubility: g/100 g H_2O)

Temp./K	273	283	293	298	303	313	323	333	353	373
Solubility	1.54	1.43	1.33	1.27	1.25	1.17	1.08	1.01	0.85	0.72

can be shown as $h = h_+ + h_- + h_G$, in which h_+ , h_- and h_G are the reduced coefficients induced by positive and negative ions and the dissolved gas, respectively. The h_G of CO_2 decreases with increasing temperature, as shown in Table 1 [16].

And h_+ and h_- values of the common ions are listed in Table 2 [16].

It can be seen from Table 2 that among the common ions, HCO_3^- has the most significant influence on the reduction of CO_2 solubility coefficient. In the system studied in this paper, LiHCO_3 is produced continuously with the progress of the reaction, and the CO_2 solubility coefficient will decrease gradually according to the principle given above. So, it can be assumed that generation of bicarbonate ions can hinder the dissolution of CO_2 which can produce reaction resistance for the whole process.

Small amounts of $\text{Li}_2\text{CO}_3(\text{s})$ can dissolve in water as shown in Table 3 [17]. However, the dissolubility data of LiHCO_3 is only limited in 291 K for $5.5 \text{ g} \cdot (100 \text{ g H}_2\text{O})^{-1}$.

In this work, we investigated the parameters influencing the dissolution of Li_2CO_3 in the CO_2 -water solution including CO_2 partial pressure, gas-bubble perforation size, CO_2 flow rate, solid concentration in the slurry, particle size of Li_2CO_3 , temperature and slurry height in the slurry bubble column reactor. The kinetic equation and the apparent activation energy were obtained.

EXPERIMENTAL SECTION

1. Experimental Setup

A 0.05 m inner diameter, 1.00 m high glass column was constructed and used for the carbonation experiments. The column has a feed hopper and an exhaust pipe at the top, and the feed hopper can also be used as a sampling point which can be shut up when it is unused. A perforated plate used as a CO_2 -bubbler is placed at the bottom of the column just above the gas inlet. The bubbler is either made of sintered glass or sand core plate.

The column was designed to be easily assembled and dissembled. A jacket at the outer side of the column was fitted with circulating water from a thermostat to control the reaction temperature. The air and CO_2 supplied by an air compressor and a CO_2 cylinder, respectively, were bubbled to a buffer vessel and then to the column with different proportions. The gas flow rates were measured with the calibrated rotameters connected between the gas cylinder orifice and the column as shown in Fig. 1. The exhaust gas was bubbled to an absorption bottle with alkaline solution through the exhaust pipe.

2. Materials and Chemicals

The crude Li_2CO_3 used in this work was extracted from salt lake brines and supplied by the Qinghai Lithium Co. Ltd. China. The physical and chemical analysis of the feedstock containing approximately 99.0% lithium carbonate is listed in Table 4.

CO_2 of high purity grade (99.5% minimum) supplied in a 12 kg cylinder was used for the carbonation process. Deionized water was

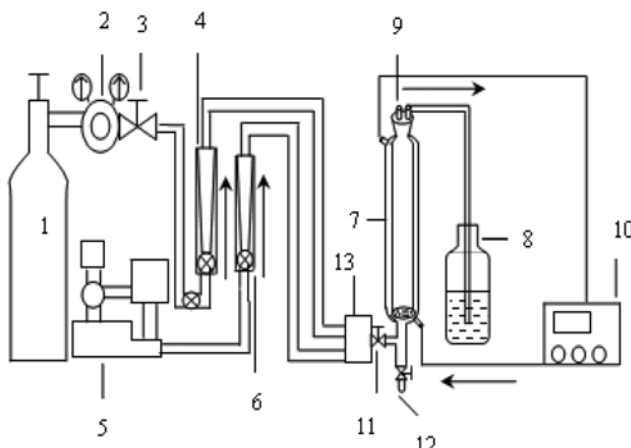


Fig. 1. Schematic diagram of the experimental setup of direct carbonation of Li_2CO_3 slurries.

1. CO_2 gas cylinder	8. Exhaust absorption bottle
2. Pressure gauge	9. Feed hopper
3. Pressure reducing valve	10. Thermostat
4. Gas rotameter	11. Gas inlet
5. Air compressor	12. Drain
6. Gas rotameter	13. Gas buffer vessel
7. Column reactor	

Table 4. Impurities contents in the feedstock

Component	wt%
Li_2CO_3	99.0
Chloride	0.1298
Sulfide	0.1352
Barium	0.0165
Boron	0.0469
Calcium	0.1112
Magnesium	0.0816
Iron	0.0009
Potassium	0.0596
Sodium	0.1017
Acid insoluble residue	0.3562

used for preparation of slurry and analytical solutions and for rinsing. Stock LiCl solution was used for calibration in atomic absorption spectroscopy (AAS) analysis.

The crude Li_2CO_3 was dried and sieved by a vibro-lab sieving machine. After sieving, each fraction with different mean mesh sizes was collected and weighed.

3. Experimental Procedure

The experimental procedure was as follows:

(1) The treated sample was accurately weighed and then immersed in the quantitative deionized water to form a slurry.

(2) Desired amount of slurry was charged into the column reactor through the feed hopper; thereafter, the hopper valve was shut.

(3) The reaction temperature was adjusted by the circulating water whose temperature was controlled by a thermostat. The air and CO_2 flows were monitored by the calibrated rotameters, and the gases should be first bubbled into a gas buffer vessel so as to maintain the pressure at 1 atm and good mixing.

(4) Slurry samples were taken through the sampling point at pre-assigned time intervals and directly filtered. A precise volume of the filtrate was taken and stored in a sealed bottle for subsequent analysis.

(6) At the end of each experiment, the air and CO_2 flows were stopped. The reactor was drained and rinsed with deionized water.

4. Method of Analysis

The filtered sample was properly diluted to a certain ratio to suit the calibration of the AAS (GBC-932 plus AAS from Australia). The AAS was calibrated using 0 to 5 mg mL^{-1} stock LiCl standards for the analysis of Li^+ . This test was a measure of the Li^+ dissolved in the slurry due to carbonation. Assuming that the source of the Li^+ is mainly from the carbonation of Li_2CO_3 , the ratio of the Li_2CO_3 conversion can be calculated using Eq. (8) according to Eq. (1).

$$X = \frac{n}{2} \frac{M_{\text{Li}_2\text{CO}_3}}{m_0} 100\% \quad (8)$$

where X is the conversion ratio of Li_2CO_3 ; n is the number of moles of dissolved Li^+ (mol); $M_{\text{Li}_2\text{CO}_3}$ is the molecular weight of Li_2CO_3 ($\text{g} \cdot \text{mol}^{-1}$); m_0 is the initial weight of crude Li_2CO_3 before carbonation (g).

RESULTS AND DISCUSSION

1. Effect of CO_2 Partial Pressure

The effect of CO_2 partial pressure on Li_2CO_3 dissolution was studied. CO_2 was bubbled into the slurry under different partial pressures, which were obtained by dilution with air. The solubility of CO_2 in water was found to increase with the increase of pressure and the decrease of temperature [18]. However, the solubility of Li_2CO_3 in water as a function of CO_2 partial pressure has never been reported till now. The Li_2CO_3 conversion increases with the increase of CO_2 partial pressure in the course of the reaction as plotted in Fig. 2. To increase the reaction rate and to eliminate the film diffusion resistance, pure CO_2 was used for the rest of the experiments.

2. Effect of Gas-bubble Perforation Size

The Li_2CO_3 conversions versus time during the carbonation pro-

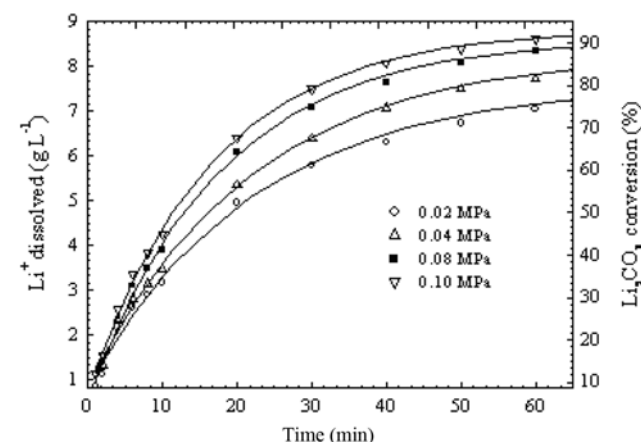


Fig. 2. Effect of CO_2 partial pressure on direct carbonation of Li_2CO_3 : 0.061 mm mean particle size, 50 g L^{-1} solid concentration, 0.08 $\text{m}^3 \text{h}^{-1}$ gas flow, porous gas distributor, 74% H/H_0 (ratio of slurry height versus column initial height), at room temperature.

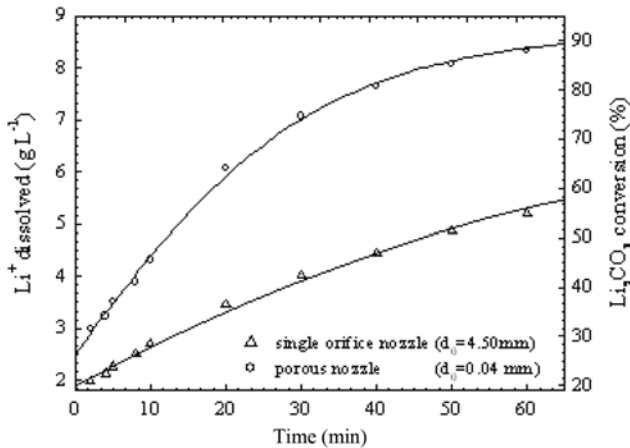


Fig. 3. Effect of gas-bubble perforation size on direct carbonation of Li_2CO_3 : 0.061 mm mean particle size, 50 g L^{-1} solid concentration, $0.08 \text{ m}^3 \text{ h}^{-1}$ CO_2 flow, 74% H/H_0 , at room temperature.

cess with different gas-bubble perforation size were obtained. The results shown in Fig. 3 indicated that the Li_2CO_3 conversion in the reactor with porous and small-orifice gas distributor was higher than that with single and big orifice, so that gas and slurry were contacting well, which was helpful to the reacting progress [19]. The porous gas distributor was used for the rest of the experiments.

3. Effect of Solid Concentration in the Slurry Mixture

The Li_2CO_3 conversions versus time for various solid concentrations are shown in Fig. 4. It can be seen that Li^+ dissolved in the system generally decreased with increasing solid concentration. The carbonation of Li_2CO_3 in the CO_2 -water is a typical non-catalytic gas-liquid-solid three phase reaction. As the solid concentration in the slurry mixture increases, the density of the slurry and the friction between phases increase [20], which may render the insufficient $\text{Li}_2\text{CO}_3(\text{s})/\text{H}_2\text{O}(\text{l})/\text{CO}_2(\text{g})$ three-phase total interfacial area. On the other hand, with the increase of solid concentration, its bulk concentration will increase, which in turn raises the bulk diffusion re-

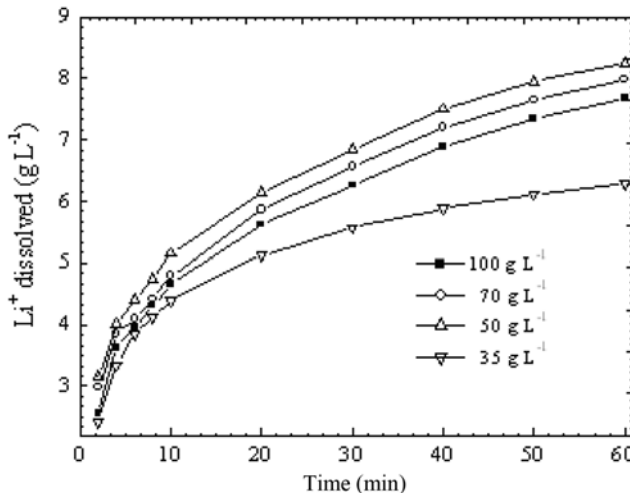


Fig. 4. Effect of solid concentration on direct carbonation of Li_2CO_3 : 0.061 mm mean particle size, $0.08 \text{ m}^3 \text{ h}^{-1}$ CO_2 flow, porous gas distributor, 74% H/H_0 , at room temperature.

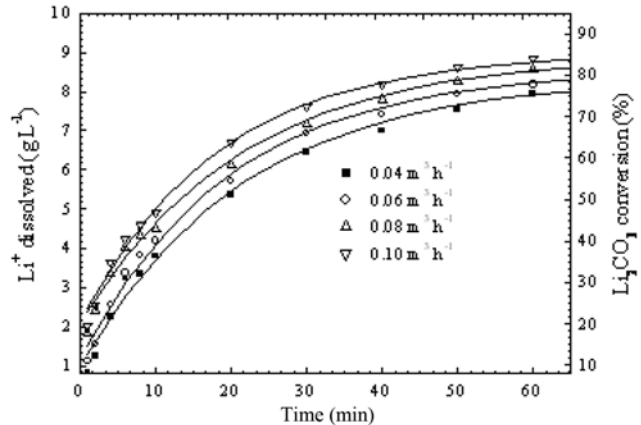


Fig. 5. Effect of CO_2 flow on direct carbonation of Li_2CO_3 : 0.061 mm mean particle size, 50 g L^{-1} solid concentration, porous gas distributor, 74% H/H_0 , at room temperature.

sistance in the liquid phase and at the liquid-solid boundary [21].

4. Effect of CO_2 Flow Rate

As shown in Fig. 5, the increase of CO_2 flow rate enhanced the Li_2CO_3 dissolution in CO_2 -water solution. It might be explained as follows: as the gas flow rate increases, the volumetric mass transfer coefficient of the gas-liquid phases increases [22]. Gas-liquid mass transfer is often accompanied by interfacial turbulence. The interfacial turbulence is caused by the non-uniformity of mass transfer, but it considerably improves mass transfer in return [23]. With the increase of CO_2 flow rate, the interfacial turbulence shall enhance, which may weaken the interfacial tension. As a result, the film boundary can be easily broken and the mass transfer coefficient increases.

5. Effect of Particle Size of Li_2CO_3

The Li_2CO_3 was sieved and the mean particle size ranged from 0.061 to 0.165 mm. The Li_2CO_3 conversions versus time for various particle sizes are shown in Fig. 6. An increase of the reaction rate with the decrease of particle size was observed, which was in accordance with the theory. As the solid particle size decreases, the total surface area of particles and the active spots of the reaction

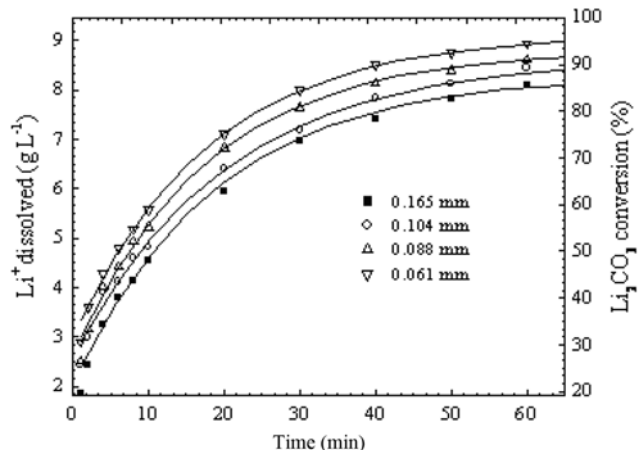


Fig. 6. Effect of Li_2CO_3 particle size on direct carbonation of Li_2CO_3 : 50 g L^{-1} solid concentration, porous gas distributor, 74% H/H_0 , $0.08 \text{ m}^3 \text{ h}^{-1}$ CO_2 flow, at room temperature.

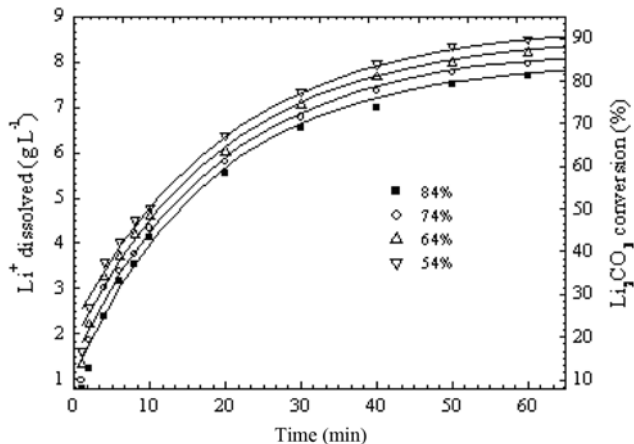


Fig. 7. Effect of slurry height on direct carbonation of Li_2CO_3 : 50 g L^{-1} solid concentration, 0.061 mm mean particle size, porous gas distributor, 0.08 $\text{m}^3 \text{h}^{-1}$ CO_2 flow, at room temperature.

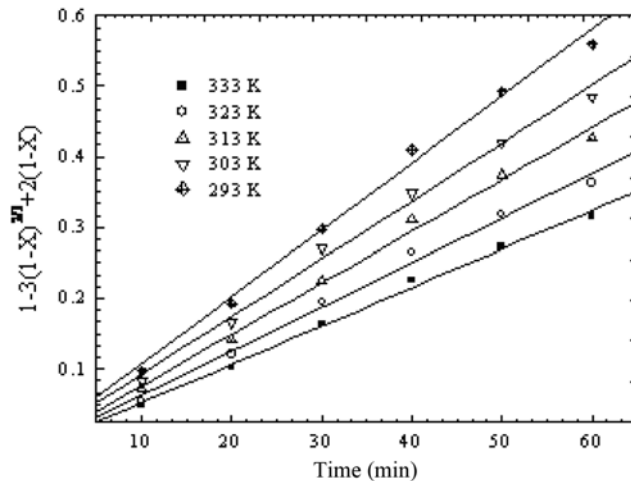


Fig. 9. Kinetics of the reaction with different temperature fitted with Eq. (9): 50 g L^{-1} solid concentration, 0.061 mm mean particle size, porous gas distributor, 0.08 $\text{m}^3 \text{h}^{-1}$ CO_2 flow, 74% H/H_0 .

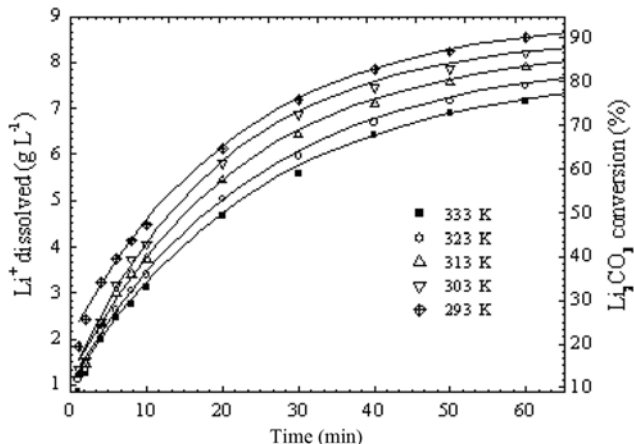


Fig. 8. Effect of reaction temperature on direct carbonation of Li_2CO_3 : 50 g L^{-1} solid concentration, 0.061 mm mean particle size, porous gas distributor, 0.08 $\text{m}^3 \text{h}^{-1}$ CO_2 flow, 74% H/H_0 .

will increase, hence the acceleration of the reaction.

6. Effect of Slurry Height in the Reactor

The effect of the ratio of slurry height versus column initial height (H/H_0) on Li_2CO_3 dissolution is shown in Fig. 7. It is clear that the dissolution rate of Li_2CO_3 increases as the height of slurry in the column decreases. When the slurry height in the column decreases, good mixing can be obtained, and CO_2 gas can be bubbled into the reactor easily with particles dispersion homogeneity under the same CO_2 flow rate; hence the reaction rate is accelerated.

7. Effect of Reaction Temperature

The effect of temperature on Li_2CO_3 dissolution is demonstrated

in Fig. 8. Fig. 8 indicates that lower temperatures are more favorable for this reaction. In general, the reaction rates increase with increasing temperature according to the Vant Hoff approximate rule [24]. But it is a somewhat more sophisticated for the carbonation of Li_2CO_3 , because the solubility of CO_2 decreases with increasing temperature and the LiHCO_3 produced decomposes at high temperatures. Room temperature is recommended.

8. Kinetics and Mechanism

Though there is no formation of solid product layer in the course of the noncatalytic reaction in this experiment, the formation of HCO_3^- can also hinder the reaction with the same effect as the solid product layer by the analysis that we mentioned above. So, there existed the product layer diffusion resistance produced by HCO_3^- in the carbonation process of Li_2CO_3 . As to the noncatalytic fluid-solid reactions, various models and equations have been proposed to describe the reaction kinetics. Among these equations, the integrated rate Eq. (9) for processes controlled by product layer diffusion (i.e., diffusion through the product layer in the reaction system) is usually tested in systems in which the reaction surface moves inwards through the particles with product layer diffusion resistance during the reaction [25-27].

$$1-3(1-X)^{2/3}+2(1-X)=kt+b \quad (9)$$

where X is the Li_2CO_3 conversion; k (time^{-1}) is the reaction rate constant of the carbonation process; t is the reaction time; and b is a constant related with the reaction.

Plots of Eq. (9) using the experimental data obtained above show that it is obeyed for a reaction time of 60 min. The data obtained at

Table 5. Parameters of the fitted curves under different temperatures

Parameters	T/K				
	293	303	313	323	333
k (min^{-1})	0.009562	0.008148	0.007013	0.006282	0.005407
Correlation coefficient	0.9954	0.9953	0.9966	0.9964	0.9977

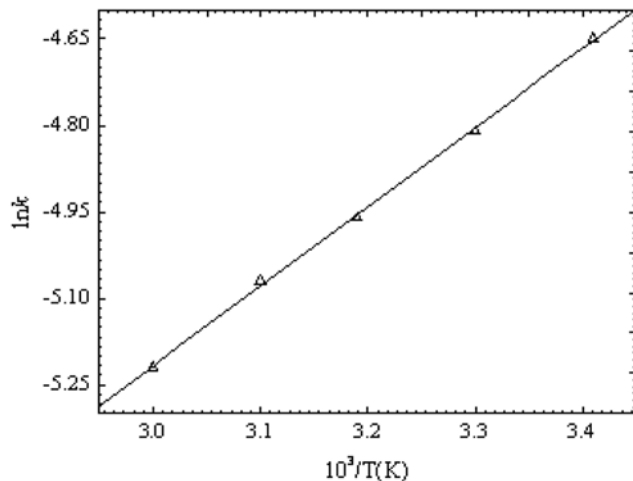


Fig. 10. Plot of $\ln k$ vs. T^{-1} (k values calculated from Fig. 9).

different temperatures were fitted with Eq. (9), and good linearity was found between $1-3(1-X)^{2/3}+2(1-X)$ and t as shown in Fig. 9.

From Fig. 9, the slopes of the straight lines, i.e., the apparent reaction rate constants k and the correlation coefficients were obtained and shown in Table 5.

On the basis of the following Arrhenius equation:

$$\ln k = -\frac{E_a}{RT} + b \quad (10)$$

where k is the rate constant; E_a is the Arrhenius activation energy ($\text{kJ}\cdot\text{mol}^{-1}$); b is a constant; R is the gas constant ($\text{J}\cdot\text{mol}^{-1}\cdot\text{K}^{-1}$); T is the temperature (K).

The reaction activation energy can be obtained by plotting $\ln k$ versus T^{-1} . Fig. 10 shows the Arrhenius plot with the reaction rate constant k calculated from Fig. 9, and the correlation coefficient of the line was 0.9996. The calculated activation energy E_a of the carbonation reaction in this paper was found to be a negative value of $-11.36 \text{ kJ}\cdot\text{mol}^{-1}$, which illuminates the dynamic complexity of this reaction. As to an elementary reaction, E_a can be given an explicit physical meaning, and it is commonly considered as the difference value of the average energy of activated molecules and the average energy of reactant molecules. While as to a complex reaction, E_a which is often called the apparent activation energy has no explicit physical meaning, and it is just the specific combination of the activation energies of each elementary reaction. The E_a here is just the apparent activation energy. And it might be also related to the physical mass transfer processes, such as the dissolution of CO_2 ; moreover, it is true that the solubilities of the reactants (Li_2CO_3 and CO_2) and the product (LiHCO_3) decrease with increasing temperature, resulting in the hampering effect of temperature on the conversion reaction. The reaction itself might have a negative temperature coefficient, hence the negative apparent activation energy.

In conclusion, refining of crude Li_2CO_3 can be easily achieved by direct carbonation with CO_2 -water solutions in a slurry bubble column reactor. And the dissolution of CO_2 is vital to the whole process.

CONCLUSIONS

This work was an extensive investigation of direct carbonation

of Li_2CO_3 slurries by CO_2 in a slurry bubble column reactor at atmospheric pressure. The process is based on the reaction of slight-soluble Li_2CO_3 with CO_2 -water solution to convert the former to water-soluble LiHCO_3 . And this process can be handled easily.

The parameters that may affect the dissolution of Li_2CO_3 in CO_2 -water solutions were investigated. The dissolution rate of Li_2CO_3 was found to increase with increasing CO_2 partial pressure inside the column reactor and CO_2 flow rate, or with decreasing temperature and slurry height in the column reactor. On the other hand, the Li_2CO_3 dissolution rate decreased with increasing the solid concentration or the Li_2CO_3 particle size. Under the appropriate conditions selected in this paper, the Li_2CO_3 conversions can reach over 90% after 60 min.

The recovery of CO_2 is possible and can be easily handled by heating the LiHCO_3 solutions under vacuum, though this part is not covered in this paper. The dissolution of CO_2 is vital to the whole carbonation process. All methods that can improve the dissolution of CO_2 in the slurry will be beneficial to the process. Room temperature is recommended, because the dissolution of Li_2CO_3 decreases with increasing temperature, but extra cost is required to run the process below room temperature.

ACKNOWLEDGEMENT

The authors would like to thank the Chinese Academy of Sciences and the Ministry of Science and Technology of China for their financial support. The authors are also indebted to those who helped in one way or another to complete this work.

REFERENCES

1. P. M. Brown, US Patent, 4,036,713 (1977).
2. P. M. Brown and C. E. Falletta, US Patent, 4,207,297 (1980).
3. K. Amouzegar, G. S. Armant and S. Harrison, US Patent, 6,048,507 (2000).
4. S. Harrison, K. Amouzegar and G. S. Armant, US Patent, 20,010,028,871 (2001).
5. G. S. Armant, K. Amouzegar and S. Harrison, US Patent, NZ504,956 (2002).
6. B. Leutner (DE), H. Friedrich (DE) and J. Pfeffinger (DE), US Patent, 6,592,832 (2003).
7. D. K. Lee, *Chem. Eng. J.*, **100**, 71 (2004).
8. A. I. Fernández, J. M. Chimenos, M. Segarra, M. A. Fernández and F. Espiell, *Hydrometallurgy*, **53**, 155 (1999).
9. F. Fang, Z. S. Li and N. S. Cai, *Korean J. Chem. Eng.*, **26**, 1414 (2009).
10. S. C. Lee, B. Y. Chio, C. K. Ryu, Y. S. Ahn, T. J. Lee and J. C. Kim, *Korean J. Chem. Eng.*, **23**, 374 (2006).
11. K. S. Hwang, S. W. Park, D. W. Park, K. J. Oh and S. S. Kim, *Korean J. Chem. Eng.*, **26**, 1383 (2009).
12. L. N. Plummer and T. M. L. Wigley, *Geochim Cosmochim. Acta*, **40**, 191 (1976).
13. R. E. Loewenthal and G. V. Maria, *Carbonate chemistry of aquatic systems: Theory and applications*, vol.1, Ann Arbor, MI (1982).
14. J. T. Edsall, in *CO₂: Chemical, biochemical, and physiological aspects*, R. E. Foster, J. T. Edsall, A. B. Otis and F. J. W. Roughton Eds., NASA, Washington DC (1969).

15. T. G. Wang and Z. H. Li, *Chem. Eng.(China)*, **33**, 39 (2005).
16. C. F. Zhang, *Gas-liquid reaction and reactor*, Chemical Industry Press, Beijing (1985).
17. C. W. Robert, *Handbook of chemistry and physics*, 55th Ed., CRC Press (1974-1975).
18. W. S. Dodds, L. F. Stutzman and B. J. Sollami, *Ind. Eng. Chem., Chem. Eng. Data Series*, **1**, 92 (1956).
19. J. Wang, Y. Mao, Y. S. Liu and R. Cao, *Chem. Eng. (China)*, **34**, 28 (2006).
20. S. H. Zhang, T. Li, B. C. Zhu and Z. B. Zhu, *J. Chem. Ind. Eng.*, **56**, 200 (2005).
21. L. N. Plummer, T. M. L. Wigley and D. L. Parkhurst, *Critical review of the kinetics of calcite dissolution and precipitation*, in: E. A. Jenne (Ed.), *Chemical Modeling of Aqueous Systems, American Chemical Society Symposium, Series*, 93, 537 (1979).
22. I. A. E. Samir, M. J. J. Anabtawi and S. L. Isaac, *Chem. Eng. Process.*, **43**, 1085 (2004).
23. Y. G Ma, X. W. Yang, H. S. Feng and K. T. Yu, *Chem. Eng. (China)*, **32**, 1 (2004).
24. X. C. Fu, W. X. Shen and T. Y. Yao, *Physical Chemistry*, 4th Ed., High Education Press, Beijing (1990).
25. J. Szekely, J. W. Evans and H. Y. Sohn, *Gas-solid reactions*, 1st Ed., Chinese Building Industrial Press, Beijing (1986).
26. H. X. Guo, *Applied chemical engineering kinetics*, 1st Ed., Chemical Industry Press, Beijing (2003).
27. H. L. Fan, CH. H. Li and K. C. Xie, *Fuel*, **81**, 91 (2002).